A Thunderstorm Bow Wave

G. CHIMONAS

Georgia Institute of Technology, Atlanta, GA 30302

CARMEN J. NAPPO

Atmospheric Turbulence and Diffusion Laboratory, Oak Ridge, TN 37831

(Manuscript received 11 April 1986, in final form 27 August 1986)

ABSTRACT

The thunderstorm solitary gust or bow wave, observed by Doviak and Ge, is examined from the viewpoint of boundary layer wave theory. It is concluded that all its well defined characteristics are consistently modeled as a bow wave of ducted atmospheric modes accompanying the traveling storm. Secondary features, such as the later onset of turbulence, the solitary echo in the radar return, and the apparent rarity of such events can also be understood through a bow wave model. It is also suggested that the radar echo return cannot be attributed to a homogeneous distribution of scattering centers, and more investigation into the actual scattering process is needed.

1. Introduction

Atmospheric waves are observed in a great variety of meteorological circumstances. Sometimes these waves are passive by-products of changing conditions, but in other cases they contribute to the processes going on around them and must be considered an important element in dynamic meteorology. Large amplitude wave events are particularly interesting since they contain information needed in so many different problems. There is the question of how well the familiar linearized theory describes the wave characteristics, and then how well the nonlinear theories fare in explaining any discrepancies. There are all the problems of the wave interaction with the background flow, including the wave generation of turbulence. There is the challenge of identifying the source of the wave. And, no doubt, many others.

This paper is concerned with a well-documented large amplitude wave observed by Doviak and Ge (1984). These authors present a dataset that allows for further detailed study. They have also presented numerous insights to help further investigations. We will demonstrate that the observations fit a bow wave emanating from a traveling storm cell, and that the wave character is determined by the ducting properties of the boundary layer. A bow wave requires a precise matching of the storm velocity to the duct characteristics. We show that even a 15% change in the storm speed or the low level winds will destroy the matching and hence eliminate the bow wave. This explains the demonstrated rarity of the event. We also suggest that nonlinearities including wave overturning, caused by the arrival of a secondary bow wave, dominate the latter part of the event. If this is so, such waves would be sporadic sources of rapid mixing in the boundary layer.

The wave system we are concerned with in this paper was observed along two special sections probed by the available apparatus. We do not have data to reconstruct a full horizontal section through the disturbance. However, analogous examples of geophysical bow waves are revealed in satellite pictures of atmospheric waves observed in the lee of small islands (Gjevik and Marthinsen, 1978; Marthinsen, 1980; see also the dynamic analysis of this event by Simard and Peltier, 1982). Although the wind in these island waves was particularly simple, being confined to a single direction, it seems likely that the event we are studying would share many of these lee-wave characteristics.

2. The event

We introduce the data by quoting from the opening paragraph of Doviak and Ge (1984):

> In the late evening of 11 May 1980, a solitary gust propagated 100 km from its thunderstorm source to be observed by NSSL's Doppler radar, a 444 meter tall meteorologically instrumented television tower, and a surface network of automated weather stations all yielding unique data on this long lasting ($\geq$1.5 h) phenomenon. . . . A time sequence of the field of thunderstorm and gust echoes (Fig. 1) suggests that the gust propagated with a nearly constant velocity of 13 m s^{-1}.

Although Doviak and Ge refer to the event as a solitary gust and include a discussion of its possible interpretation in terms of solitary wave theory, they do

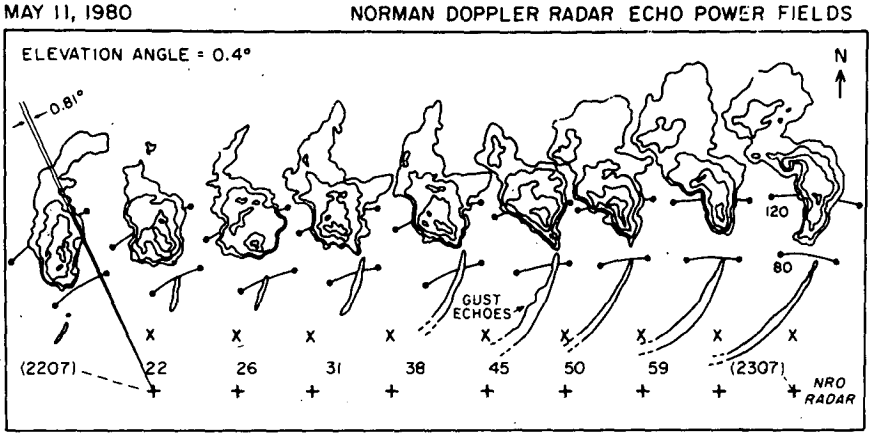

FIG. 1. A one-hour sequence of radar observations of the storm and its associated bow wave. Sequence begins at 2207 local time. The + indicates the position of the Doppler radar, the × marks the tall tower. Range arcs are shown at 80 and 120 km. (Doviak and Ge, 1984).

not rule out the possibility of other wave interpretations. Most of their remarks are made in more general terms, and address the need to examine other viewpoints. A previous presentation of the radar records describes it as a solitary bow accompanying the storm cell (Rust and Doviak 1982). It will be suggested later that the radar shows only a single crest because it is unable to resolve the rest of the wave activity. The tower shows more of the wave train. Whatever, apart from the "solitary" it is clear that Doviak and Ge consider the bow wave as one possible model. This is the route we will follow.

Figure 2 reproduces data from the tall tower. The turbulence recorded after 2320 is subject to several interpretations. Doviak and Ge suggest that it is generated by the wave disturbance, a viewpoint with which we agree. But they seem to propose that the wave is confined to the period immediately prior to the turbulence, and that the wave passage has left behind it a mean profile that is dynamically unstable and hence turbulent. We feel that it is more likely that the wave activity extends through the entire period of disturbance and creates the turbulence by its immediate distortions of the flow. This is in keeping with the ideas of wave overturning in the higher regions of the atmosphere (Hodges 1967, Lindzen 1981, Fritts 1985). It also implies that the wave distortion of the flow maximizes at, or just after, the onset of the turbulence. The bow wave concept offers a simple explanation, presented later, for such behavior.

Either way the wave is supplying energy for the creation of the turbulence, whose vigor and duration suggest that an isolated (solitary) wave would soon decay away. This is in stark contrast with the observations, providing preliminary evidence that the wave is being constantly generated, as in a bow wave.

Figures 3 and 4 show the wind and temperature fields as far as Doviak and Ge could determine them at the time of the event. They estimate that the storm traveled towards 58° at 23 m s^{-1}, while the wave front propagated towards 132° at a speed of about 13 m s^{-1}, Fig. 5. No estimates of probable errors in these numbers are given.

3. Formulation of the bow wave

A bow wave is formed when a disturbance moves through a medium faster than some wave component

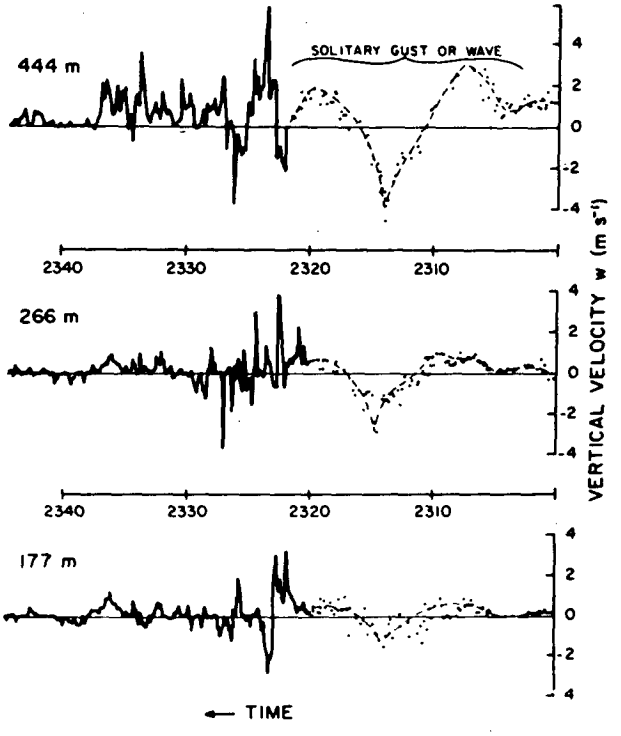

FIG. 2. Vertical velocity record from three levels of the tall tower during passage of the wave. (Doviak and Ge, 1984).

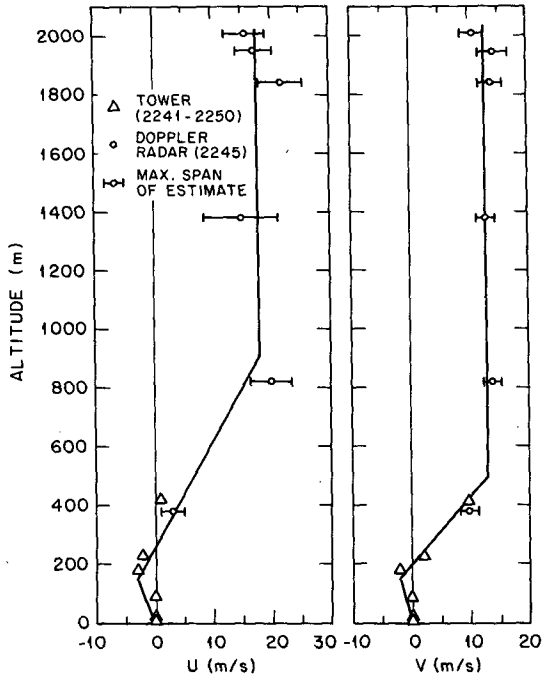

FIG. 3. Wind profiles used in the model calculations (solid lines) and the observed data points; U is the north–south component, V is the east–west component.

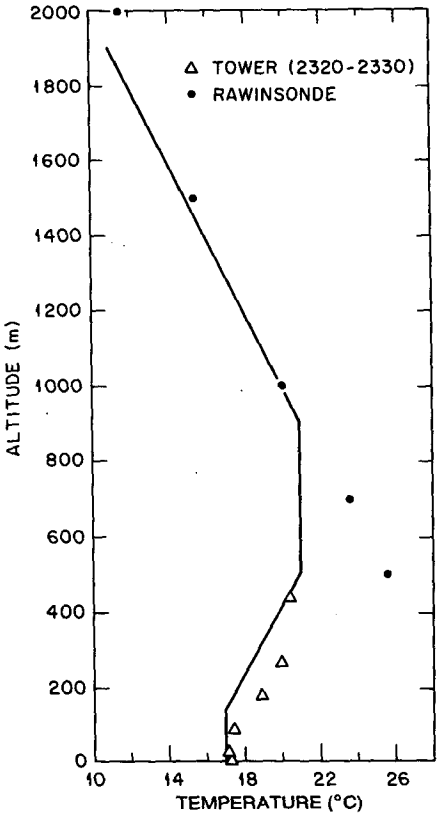

FIG. 4. Temperature profile used in model calculations (solid line) and data points from observations. The dotted line is the rawinsonde record from OKC released at 1800 UTC 11 May 1980.

supported by the medium. Familiar examples include the waves accompanying ships (or swimming ducks) and the sound shock associated with a supersonic aircraft. Mountain lee waves are essentially the same phenomenon, but we usually choose to think that the mountain is at rest while the medium does the moving. Somewhat perversely it is often easier to formulate the bow wave problem in a frame of reference that moves with the disturbance, turning it into a lee-wave type of problem.

The steady state condition, in which the disturbance has constant form and velocity in a uniform medium, is much easier to solve than less idealized time dependent or spatially inhomogeneous problems. Our work is a steady state study. It gives a useful approximation for the rather slowly varying conditions of the observations. There are three steps in the analysis. First, we must identify the wave properties of the medium. Then we must consider the implications and restrictions of bow wave formation. Finally, we must consider the wave breaking.

The wave properties are defined by the wind and stratification profiles of the atmosphere. It is clear from the time scales of the disturbance that we need not be concerned with acoustic waves, and incompressible Boussinesq theory is appropriate. The large amplitude of the event suggests that it consists of modes ducted in the lower atmosphere. Such modes have a dual advantage over waves that propagate freely into the upper atmosphere, in that they are resonantly excited by the source mechanism and then confine all their energy to the lower regions where the observations are made. Many different types of mode have been identified. They range from the fast traveling Lamb waves and acoustic modes to internal gravity waves trapped by temperature structures, jets and critical levels. (Francis, 1973; Gossard and Hooke, 1975; Ley and Peltier, 1981; Lindzen and Tung, 1976; Chimonas and Hines, 1986). In the present case we find that low speed internal

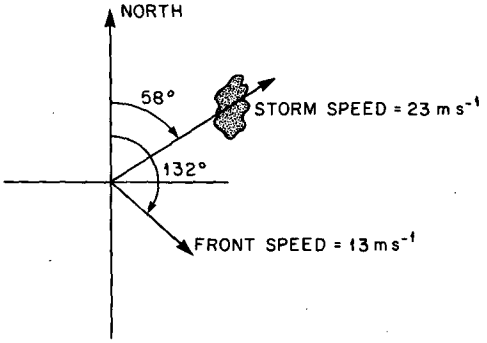

FIG. 5. Parameters of storm and wave movement deduced by Doviak and Ge.

gravity wave modes, confined to the boundary layer and free of any critical level interactions, best fit the situation. Take a set of Cartesian coordinates with z measured in the upwards vertical direction. We use the usual set of approximate linearized equations for low phase speed waves:

$$\rho_0\left[\left(\frac{\partial}{\partial t}+\mathbf{V}_0\cdot\nabla\right)\mathbf{V}_1+\mathbf{V}_1\cdot\nabla\cdot\mathbf{V}_0\right]=-\nabla p_1+\rho_1\mathbf{g} \quad (1)$$

$$\nabla\cdot\mathbf{V}_1=0 \quad (2)$$

$$\left(\frac{\partial}{\partial t}+\mathbf{V}_0\cdot\nabla\right)\rho_1-\frac{N^2}{g^2}\rho_0\mathbf{V}_1\cdot\mathbf{g}=0. \quad (3)$$

A subscript 0 indicates a mean flow value, while a subscript 1 indicates a wave field; $\mathbf{V}$ is velocity, p pressure, ρ density, g the acceleration due to gravity and N is the Brunt–Väisälä frequency,

$$N^2=g(0.0096-T')/T \quad (4)$$

where T is the temperature in degrees Kelvin and the MKS system of units is used. Here, and throughout the paper, the prime notation will be used to denote a derivative with respect to the vertical coordinate z; that is, $T'=dT/dz$.

Horizontal coordinates are defined with positive x towards the east, and hence positive y towards the north. Using the unit vector notation of a hat, the winds have component forms

$$\mathbf{V}_0=\hat{x}U+\hat{y}V \quad (5)$$

$$\mathbf{V}_1=\hat{x}u_1+\hat{y}v_1+\hat{z}w_1 \quad (6)$$

U and V are functions of z only. We now take Fourier transforms in x, y and t of the Eqs. (1)–(3), and consider a particular component of the wave field,

$$(u_1,v_1,w_1,\rho_1,p_1)=(u,v,w,d,p)\exp i(\omega t-\mathbf{k}\cdot\mathbf{r}) \quad (7)$$

where u, v, w, d and p are functions of z only, and $\mathbf{r}$ is vector position in the horizontal plane. The equations (1)–(3) yield a set of linear simultaneous equations in the wave amplitudes that can be manipulated to yield the differential equation governing w:

$$w''+(\rho_0'/\rho_0)w'+\left[\frac{N^2k^2}{(\omega-\mathbf{k}\cdot\mathbf{V}_0)^2}+\frac{U''k}{(\omega-\mathbf{k}\cdot\mathbf{V}_0)}-k^2\right]w=0. \quad (8)$$

The term in w' is of no consequence for most boundary layer wave work, including the present problem, so although it can be kept without adding any significant computational difficulty, we follow standard procedure and drop it to obtain the Taylor-Golstein equation

$$w''+\left[\frac{N^2k^2}{(\omega-\mathbf{k}\cdot\mathbf{V}_0)^2}+\frac{U''k}{(\omega-\mathbf{k}\cdot\mathbf{V}_0)}-k^2\right]w=0. \quad (9)$$

Note that in (8) and (9) the mean wind enters through $\mathbf{k}\cdot\mathbf{V}_0$. That is, only the wind component in the direction of wave propagation enters the equation. This component changes with the wave azimuth, so the propagation characteristics will also change with wave direction in the horizontal. This would not be the case in a simpler windless model atmosphere.

An idealized ducted wave obeys two boundary conditions. The atmosphere must remain in contact with the earth's surface, so w must be zero at this height. And the wave must be trapped in the lower atmosphere, with no energy loss towards $z=+\infty$. In model calculations this is achieved by requiring w to decay exponentially in a uniform upper half-space set above the planetary boundary layer structure. It is recognized that the real atmosphere does not supply convenient uniform upper half spaces, and accordingly the model results must always be used with caution. Some discussion of the "integrity" of model ducts is given in Chimonas and Hines, 1986.

The profiles used in our calculations are shown in Table 1. These are shown superimposed on the data in Figs. 3 and 4. The half-space above 900 meters contains a constant wind and lapse rate. This simple model fits the data within the rather large experimental uncertainties. It must be pointed out that at a range of 50 km the radar beam senses a 600 m vertical section of the atmosphere. The data points recorded in the wind figures are thus average values for deep adjacent layers. There is no need (or justification) to use more complex model profiles, but the particular values chosen to define them must be critically questioned. We have found that some of the modal properties are very sensitive to the values used for the winds in one height range. The model given above is the one chosen for our calculations before this became apparent. It does not optimize the agreement between the bow-wave theory and the observations. We feel that the best approach is to use the nonoptimized profiles and then consider the way results change over an allowed range of wind values. It becomes clear that available observing systems do not have the sensitivity demanded by linear wave theory. The requirements of nonlinear theory are still less attainable.

Equation (9) and the two boundary conditions provide an eigenvalue problem in the space $\{\omega, \mathbf{k}\}$. It is solved numerically. A particular value of $\mathbf{k}$ is selected, and the corresponding eigenvalue $c=\omega/k$ is sought.

TABLE 1. Wind profiles.

U (m s^{-1})	V (m s^{-1})	T (°C)	Height (m)
$-0.020z$	$-0.013z$	17	$0<z<150$
$0.028z-3$	$0.043z-2$	$17+0.0114z$	$150<z<500$
$0.028z-3$	13	21	$500<z<900$
18	13	$21-0.010z$	$900<z$

We start by scanning a likely range of c values. For a point in this range the equation is integrated from $z = 0$ (with $w = 0$) up to the height where the overlying uniform half-space begins. Here the solution is matched to a linear combination of the two known analytic wave forms by demanding continuity of pressure and displacement. The parameters c and $\mathbf{k}$ must be confined so that these upper level waves can be expressed as real exponential functions of z, one of which grows with height, the other decays. An eigensolution occurs when the matching requires only the decaying wave, so the amplitude found for the growing component measures how far the value of c is from being an eigenvalue. If we scan a range of c and find that this unwanted amplitude changes sign, we know that it has a zero in the range. An iterative procedure allows us to locate this zero, and consequently the eigenvalue c. The procedure is then repeated for a new value of $\mathbf{k}$, allowing the progressive discovery of the entire $\{c, \mathbf{k}\}$ eigenvalue curve (often called the dispersion relation). Once the first eigenvalue is found the procedure becomes very rapid.

4. The modes

Equation (9) involves the wind component in the direction of wave propagation. As shown in Fig. 6 this changes dramatically with wave azimuth. It therefore seems best to first introduce the dispersion relation obtained if we set the wind to be zero in the model and just have ducting in the temperature field. Now the atmosphere is isotropic in the horizontal and only the magnitude of the wave vector enters the problem. Figure 7 shows the modal phase speeds plotted against wave number in this simplified system. Two such curves are shown, one for the gravest mode, the other for the mode with one node in its vertical velocity field. Samples of these modes are shown in Fig. 8. There is, in fact, an infinite sequence of such modes, each with one more node in its vertical profile than its predecessor (e.g., see Chimonas and Hines 1986).

We now examine the wave dispersion when the model wind of Fig. 3 is retained. The $\{c, \mathbf{k}\}$ relation

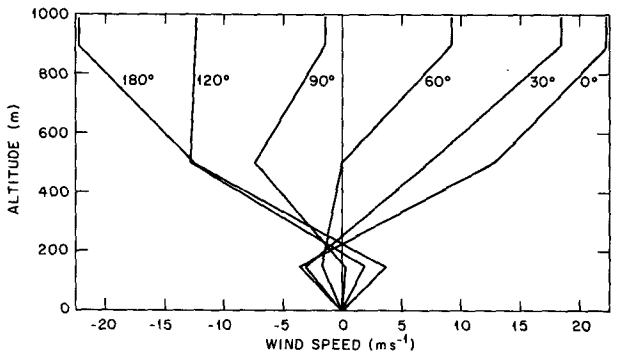

FIG. 6. Model wind component for a sequence of azimuths relative to the storm direction (58°).

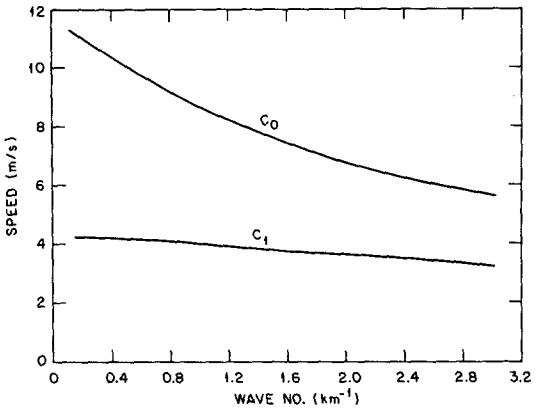

FIG. 7. The phase velocities of the fundamental (C_0) and one-node (C_1) modes of the pure temperature duct.

now defines a surface in three dimensions. Two dimensional curves may be drawn if we select a particular direction of propagation and consider how c varies as a function of wavenumber amplitude for waves in this plane. Figure 9 shows one such curve for the fundamental mode. The most obvious difference between this curve and the corresponding curve for the temperature duct, Fig. 7, is the different limiting speeds of the large wave numbers. With temperature alone this limiting speed is zero, while with the wind included in the model it is about 10 m s^{-1}. Examination of Fig. 6 shows that this is just about the maximum wind speed in this plane. This is the expected behavior of modes in an atmosphere containing a wind maximum, as is explained in Chimonas and Hines (1986).

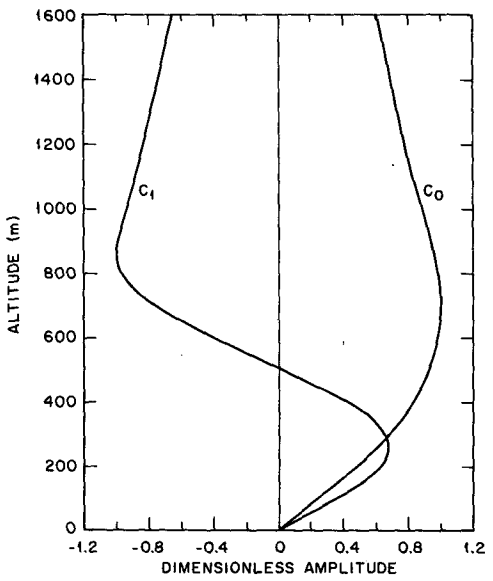

FIG. 8. Wave forms for sample modes of the temperature duct. Vertical wave velocity is shown. Fundamental mode parameters are $c = 9.5$ m s^{-1}, $k = 0.6$ km^{-1}, one-node mode parameters are $c = 4.1$ m s^{-1}, $k = 0.6$ km^{-1}.

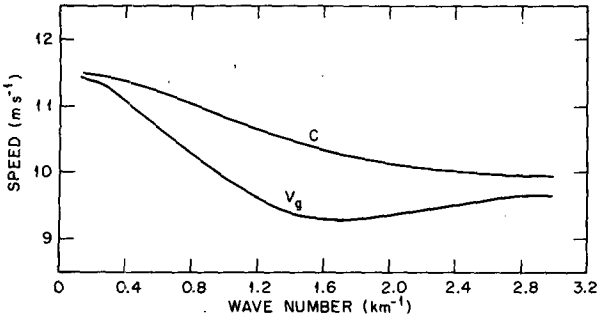

FIG. 9. Phase and group velocities of fundamental mode in the full wind and temperature duct. Mode is propagating at an angle of 60° to the storm direction (118° Magnetic).

Figure 10 shows the vertical profile of a selected mode. It may be compared with that found in Fig. 8. It is seen that in this case the wind enhances the ducting of energy into the lower boundary layer. The discontinuities in slope of the wave profile occur at the same heights as the discontinuities in slope of wind in our model. If we made the wind change smoothly (with continuous second derivatives) over a small interval, the modes would not have such discontinuities. However, their profiles would otherwise be identical, with the same slopes on either side of the small interval. This can be shown by considering the integration of (9) over the small interval where the wind slope changes.

Dispersion curves can be obtained for any desired azimuth. They all have the same general features as

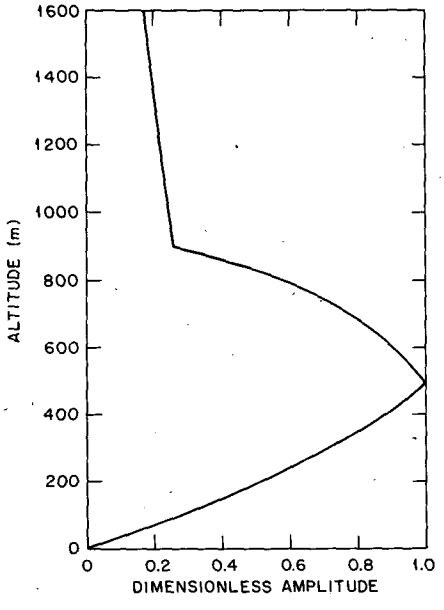

FIG. 10. Wave form of sample fundamental mode for full wind and temperature duct. Vertical wave velocity is shown. Mode parameters are $k = 0.6$ km^{-1}, $c = 11.3$ m s^{-1}, propagation direction at an angle of 60° to storm direction.

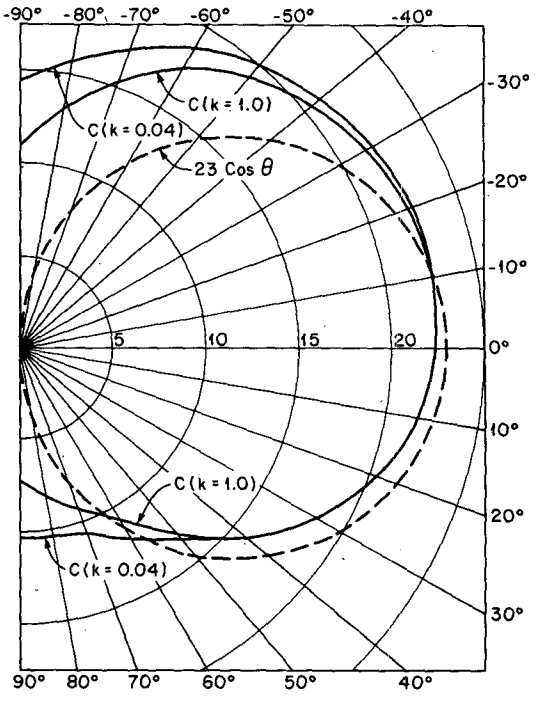

FIG. 11. Polar plot of mode characteristics for fundamental modes of full boundary layer duct. We show curves for the modes at $k = 0.04$ km^{-1} and $k = 1.0$ km^{-1}. The third curve is for 23 cosθ, the projection of the storm speed onto the wave direction.

Fig. 9. However, the properties of greatest importance in the bow-wave considerations are shown in Fig. 11. This is a polar plot showing the phase speed of the fundamental mode of wavenumber 0.04 km^{-1} against azimuth, together with a second curve for the phase speed of the relatively small-scale mode at wavenumber 1 km^{-1}. We have found that a dispersion curve drawn for any selected direction of propagation shows that the speed of the mode decreases with wave number. So Fig. 11 shows the speed range of all the modes faster than the mode at wavenumber 1 km^{-1}. The atmospheric winds conspire to bring the two curves quite close together.

5. Formation of bow waves

A bow wave is formed when a disturbance moves with sufficient speed through a wave-supporting medium. The process is readily explained by an example of waves on a pond. If a pebble is dropped into the pond it creates a circular pattern of waves that spreads with some characteristic speed C. Now suppose a series of pebbles is dropped along a straight line, with the time interval DT between successive pebbles being related to their separation DX as $DX = U \cdot DT$. A series of wave patterns resembling Fig. 12 is created. These interfere to produce a complicated pattern of crests and troughs. However, the pattern has one obvious characteristic. If U is greater than C the pattern just

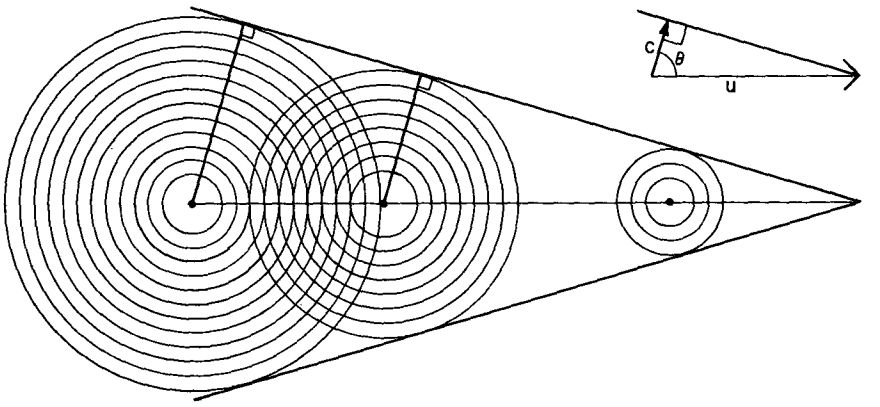

FIG. 12. The interference pattern produced by a regular sequence of staggered cylindrical wave fronts. The bow wave is defined by the limiting cone tangent to the leading wave fronts.

fits inside a cone of half angle (90°-θ) where θ is the angle between the line of disturbance and the direction of propagation of the wave front, given by $\theta = \cos^{-1} C/U$. As the interval between pebbles is made very small this cone comes to be solidly defined by the wave front of the total disturbance. This first bow wave is usually the clearest. Subsequent interference maxima exist, but dispersion and noise can obscure them.

If the speed U associated with the line is less than the propagation speed C a completely different pattern is formed. The circular front surrounding the first pebble encompasses all subsequent disturbances. There are no obvious aspects to the interference pattern which is complicated and time dependent. This is important to the storm problem because the corresponding speeds are barely able to allow the bow-wave situation.

The moving storm also forms such patterns if conditions are right. The storm disturbs the atmosphere as it modifies momentum, mass, and heat distributions. If the storm has a fixed intensity and shape these disturbances can be represented as some instantaneous function

$$F(x, y, z) = \int_{-\infty}^{\infty} \int_{-\infty}^{\infty} dk_x dk_y \tilde{F}(k_x, k_y, z) \exp i(k_x x + k_y y). \tag{13}$$

As this moves through the atmosphere with velocity U in the x direction it provides a forcing function

$$\mathcal{F}(x, y, z, t) = F(x - Ut, y, z)$$
$$= \int_{-\infty}^{\infty} \int_{-\infty}^{\infty} dk_x dk_y \tilde{F}(k_x, k_y, z) \exp i(k_x x - k_x U t + k_y y). \tag{14}$$

How the atmosphere responds to this depends very much on whether it can support free disturbances with characteristics $\exp i[k_x(x - Ut) + k_y y]$. If it does not, the surrounding medium at distances exceeding a few storm diameters will not be noticeably affected. However, if a wave mode with such characteristics does exist it will be resonantly excited and will travel out into the surrounding medium to contribute to a bow wave. Note that we have not explicitly mentioned the vertical form of the forcing function $\tilde{F}(k_x, k_y, z)$, or the vertical structure of the atmosphere. The latter enters in the calculations of the wave modes, as in the previous section. The former determines how well the forcing matches the modes, and enters the problem through overlap integrals on z if response amplitudes are explicitly calculated.

In the immediate problem we are restricted to qualitative properties. Foremost is whether such a modal response occurs in the observed storm conditions. We have drawn the curve $U\cos\theta$ in Fig. 11 with $U = 23$ m s^{-1}, the observed storm speed. Where this intersects a modal dispersion curve $C(k, \theta)$ the bow wave matching condition is satisfied.

We see that in the present model there are intersections in very narrow bands of angles about 60° and 351°. So the bow wave is not symmetric about the direction of storm motion and should take the shape shown in Fig. 13. The asymmetry results from the wind system that blows across the storm. Only the bow wave to the south of the storm was observed, and this was reported by Doviak and Ge to make an angle θ of about 74°, not significantly different from our value of 60°. The phase speeds of the group of modes that satisfy the intersection with $U\cos\theta$ in Fig. 11 fall in the range 11.2 ± 1 m s^{-1}. From Fig. 9 we see that the phase speed 11.2 m s^{-1} corresponds to a wave number of 0.6 km^{-1}, and hence a period of 15 min. This is within the limits of observation for the first peak to peak time interval seen in the tower record Fig. 2. Considering the uncertainties in the observations and the model fit we feel that the overall agreement is excellent.

Looking at Fig. 11 we observe that the storm only just manages to create the bow wave. If it had moved just a few meters per second more slowly the curve $U\cos\theta$ would lie inside the polar range plots and no

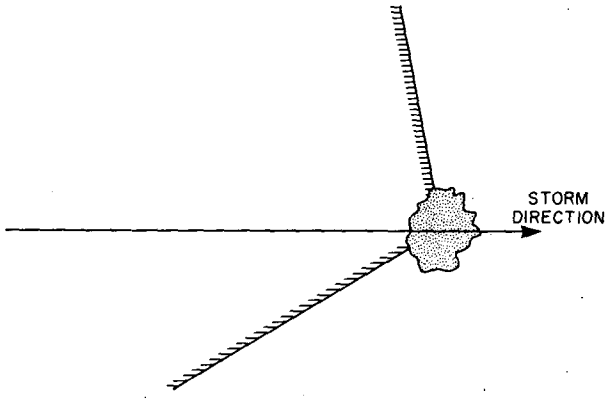

FIG. 13. The bow waves formed by the fundamental modes keeping pace with the storm. The wind field causes an asymmetry between the two arms of the bow.

intersections would occur. Or equivalently, if the wind strength everywhere had been greater by a like amount the effect would have been the same. In fact, Doviak and Ge report that a prior storm passed through the area a few hours earlier than the one observed with the bow wave. As far as they could determine the two were identical, but only the second had an associated wave. A few meters per second difference in speed, barely a 15% variation, could explain this.

The modal intersections given by Fig. 11 allow wavenumbers from zero (the fastest waves) to the plotted limit 1 km^{-1} (the slowest). If they are generated, all these, and the slower waves not yet considered, will be found in the disturbance far from the storm. The longer wavelengths arrive first, and define the leading part of the bow wave. However, we expect very little contribution from the very longest wavelengths, since the storm dimensions are usually of the order of 10 kilometers. The regions of strong interaction in the storm could be considerably smaller. This means that the forcing spectrum $\tilde{F}$ of Eq. (13) should have a well-defined peak at corresponding wavenumbers. This is consistent with the wavelength $2\pi/k = 9$ km examined above, but it also means that the disturbance is not one pure mode but a continuum of modes with a range of parameters.

Up to this point we have discussed the bow wave composed from the gravest family of modes, and the leading wavelike disturbance in the observations. Figure 2 shows that the latter half of the tower record is composed of high amplitude irregular disturbances, referred to by Doviak and Ge as turbulence. Theoretically there will be a second independent bow wave formed from the next family of modes (those with one node in their vertical velocity profile). It can be speculated that this second bow wave arrives at the beginning of the turbulent period. The two bow waves interfere producing large amplitude vacillations, wave overturning and turbulence.

To support this speculation we began computing the properties of the second bow wave. A simple geometrical calculation shows that the sequence of arrivals at the tower can be satisfied if the second bow wave front propagates at 70° with respect to the storm; that is, its cone is 10° sharper than the first one. This in turn requires a phase speed of 7.8 m s^{-1}, quite reasonable considering the greater speeds found for the fundamental modes.

However, the calculations proved to be too sensitive to the models used for the wind. With the profiles previously used the wave speeds were too small by a factor of four. But we can construct profiles that are well within the experimental limits and obtain the desired phase speeds while still maintaining the primary bow-wave characteristics. This happens as follows. The temperature ducting alone produces a wave phase speed of around 4.5 m s^{-1} for the second family (Fig. 7). We can gauge the effect of wind on the mode speed by assuming that the mode is advected by the mean wind in the vicinity of the temperature inversion (Fig. 4). With the wind model previously used, Fig. 6 indicates an adverse wind of 3 m s^{-1}, leaving a net speed of only

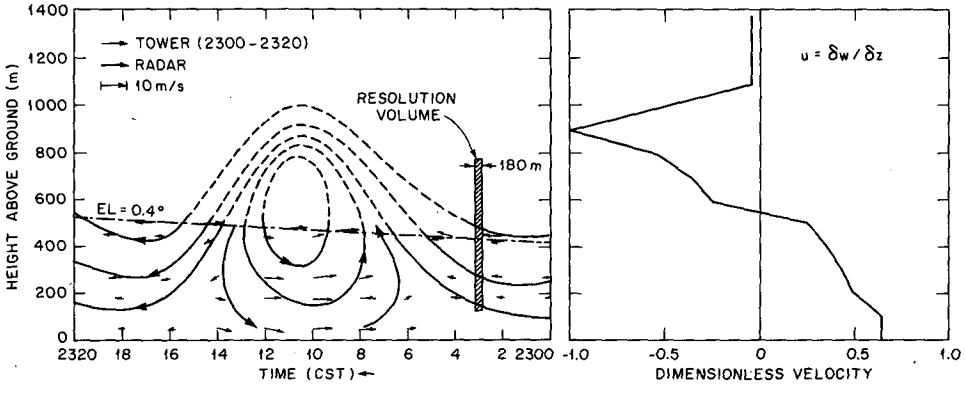

FIG. 14. Wave fields from tower observation, radar record and model calculation. The model field is shown as block averages over 100 m intervals. The vertical extent of the radar beam is also shown. (From Doviak and Ge 1984, with additions from our calculations)

1.5 m s^{-1} for the wave propagation relative to the observer. But the uncertainties in the reported winds, Fig. 3, allow us to choose models with a wind that enhances the wave speed by up to 4 m s^{-1}, giving net speeds of over 8 m s^{-1}.

With such an allowed range, fitting the observations is possible but futile. The only valid conclusion we can draw is that our hypothesis concerning the second bow-wave component does not violate the data, but much better data is needed to properly test it. Indeed we will end this paper by pointing out a serious and puzzling feature of the radar data. Figure 14 is a composite showing the winds measured at the tower as the wave passed by, the winds deduced from the radar observations of the bow wave, and the horizontal velocity field of our calculated mode. Tower and mode agree to the wave form, with a sign change for the horizontal wave disturbance just above 400 m. The radar reports a larger velocity and moreover this is supposedly an average over the indicated radar beam height. If the radar were indeed to uniformly sample the wave field, it would return about zero net result as the beam just spans a complete oscillation of horizontal velocity. This is true for both the calculated mode and the pattern hypothesized by Doviak and Ge. It might then be speculated that the radar return comes preferentially from the high flow speed portion of the atmosphere. Perhaps in this region there is strong generation of the necessary scattering centers. This may help explain why the radar shows only a single band while the theory and the tower suggest considerably more extensive activity. Whatever, it needs further investigation by the radar people.

Acknowledgments. We are indebted to Drs. Doviak and Ge for their generosity in providing us with access to their data and valuable insights into its interpretation. This work was partially supported by the National Science Foundation under Grant ATM-8519883.

REFERENCES

Chimonas, G., and C. O. Hines, 1986: Doppler ducting of atmospheric gravity waves. *J. Geophys. Res.*, **91,** 1219–1280.

Doviak, R. J., and R. Ge, 1984: An atmospheric solitary gust observed with a Doppler radar, a tall tower and a surface network. *J. Atmos. Sci.*, **41,** 2559–2573.

Francis, S. H., 1973: Lower atmospheric gravity modes and their relation to medium-scale traveling ionospheric disturbances. *J. Geophys. Res.*, **78,** 8289–8295.

Fritts, D. C., 1985: A numerical study of gravity wave saturation: nonlinear and multiple effects. *J. Atmos. Sci.*, **42,** 2043–2058.

Gjevik, B., and T. Marthinsen, 1978: Three-dimensional lee-wave pattern. *Quart. J. Roy. Meteor. Soc.*, **104,** 947–957.

Gossard, E. E., and W. H. Hooke, 1975: *Waves in the Atmosphere,* Elsevier, 456 pp.

Hodges, R. R. Jr., 1967: Generation of turbulence in the upper atmosphere by internal gravity waves. *J. Geophys. Res.*, **72,** 3455–3458.

Lindzen, R. S., 1981: Turbulence and stress due to gravity wave and tidal breakdown. *J. Geophys. Res.*, **86,** 9707–9714.

——, and K. K. Tung, 1976: Banded convective activity and ducted gravity waves. *Mon. Wea. Rev.*, **104,** 1602–1617.

Ley, B. E., and W. R. Peltier, 1981: Propagating mesoscale cloud bands. *J. Atmos. Sci.*, **38,** 1206–1219.

Marthinsen, T., 1980: Three-dimensional lee waves. *Quart. J. Roy. Meteor. Soc.*, **106,** 569–580.

Rust, W. D., and R. J. Doviak, 1982: Radar research on thunderstorms and lightning. *Nature,* **297,** 461–468.

Simard, A., and W. R. Peltier, 1982: Ship waves in the lee of isolated topography. *J. Atmos. Sci.*, **39,** 587–609.